

Non-Hermitian fractional quantum Hall states

Tsuneya Yoshida,¹ Koji Kudo,¹ and Yasuhiro Hatsugai¹

¹*Department of Physics, University of Tsukuba, Ibaraki 305-8571, Japan*

(Dated: February 28, 2022)

We demonstrate the emergence of a topological ordered phase for non-Hermitian systems. Specifically, we elucidate that systems with non-Hermitian two-body interactions show a fractional quantum Hall (FQH) state. The non-Hermitian Hamiltonian is considered to be relevant to cold atoms with dissipation. We conclude the emergence of the non-Hermitian FQH state by the presence of the topological degeneracy and by the many-body Chern number for the ground state multiplet showing $C_{\text{tot}} = 1$. The robust topological degeneracy against non-Hermiticity arises from the many-body translational symmetry. Furthermore, we discover that the FQH state emerges without any repulsive interactions, which is attributed to a phenomenon reminiscent of the continuous quantum Zeno effect.

Introduction. — In these decades, a variety of novel phenomena have been discovered which arise from topological properties in the bulk [1–13]. In particular, the topological ordered phases [14] exhibit striking topological phenomena because of correlation effects and the topological properties. One of the representative examples of topological ordered phases is a fractional quantum Hall (FQH) phase [15–17] or a fractional Chern insulator [18–23] which hosts anyons obeying fractional statistics due to the topological degeneracy of the ground states. The platforms of topological ordered phases extend to bosonic or spin systems. The toric codes for two- [24, 25] and three-dimensional systems [26] exemplify the emergence of topological ordered phase in spin systems whose relevance of correlated compounds has been discussed recently [27, 28]. These topological ordered phases also attract much attention in terms of application to the quantum computations.

Along with the above progress, recent development of technology has pioneered a new type of topological systems, non-Hermitian topological systems. Extensive studies in these years have discovered various intriguing phenomena described by topological properties of quadratic non-Hermitian matrices. For instance, it has been elucidated that non-Hermiticity may induce a topological phase which does not have its Hermitian counterpart [29, 30]. Furthermore, non-Hermiticity induces novel gapless excitations in the bulk (e.g., exceptional points [31–36], symmetry-protected exceptional rings [37–43] etc.) which arise from the defectiveness of the Hamiltonian. In addition, non-Hermiticity may induce a unique bulk-boundary correspondence [44–48] due to the non-Hermitian skin effect.

The above two progresses pose the following crucial question: what are impacts of non-Hermiticity on topologically ordered phases? In particular, it is considered to be significant to elucidate the fate of the topological degeneracy which is source of anyons for Hermitian cases. In spite of such significant open questions, there are few works addressing non-Hermitian topological ordered phases.

In this paper, we address the above issue, providing a new direction in the study of non-Hermitian topological phases. In particular, we consider a FQH system with non-Hermitian interactions which is considered to be relevant to cold atoms coupled with the environment. Our analysis based on the numerical diagonalization elucidates that the topological degeneracy is robust against non-Hermitian two-body interactions, which arises from many-body translational symmetry. Combining the topological degeneracy and direct computation of the Chern number for the ground state multiplet $C_{\text{tot}} = 1$, we end up with the conclusion that the non-Hermitian Hamiltonian shows the FQH state. Furthermore, we discover a novel phenomenon for which non-Hermiticity is essential; the FQH state emerges without the repulsive interactions. We find that this intriguing phenomenon arises from interplay between the kinetic term and the dissipative interactions which is reminiscent of the continuous quantum Zeno effect. This unconventional mechanism of the bulk gap may provide a new way to access exotic topological ordered phases.

Set up. — The non-Hermitian Hamiltonian analyzed in this paper is shown in Eq. (3) which is considered to be relevant to cold atoms. In order to see this, we start with a Hermitian FQH system which is decoupled with the environment. After that we take into account the coupling with the environment, yielding a non-Hermitian Hamiltonian.

Firstly, we note that the following FQH systems of a square lattice may be realized for cold atoms

$$H_0 = - \sum_{\langle i,j \rangle} t_0 e^{i\phi_{ij}} c_i^\dagger c_j + V_R \sum_{\langle i,j \rangle} n_i n_j. \quad (1)$$

Here, c_i^\dagger creates a spinless fermion at site $i = (i_x, i_y)$ of the two-dimensional system. If necessary, we rewrite c_i^\dagger as $c_{i_x i_y}^\dagger$. t_0 denotes the hopping between sites. The phase factor ϕ_{ij} describes the flux penetrating the plaquet. In this paper, we employ the string gauge [49] (see Fig. 1). We define the flux density as $\phi := N_\phi / N_x N_y$ where N_ϕ denotes the number of flux quanta penetrating the $N_x \times N_y$ -square lattice. The filling factor is de-

defined as $\nu := N_f/N_\phi$ where N_f denotes the number of fermions. For fabrication of the above system with cold

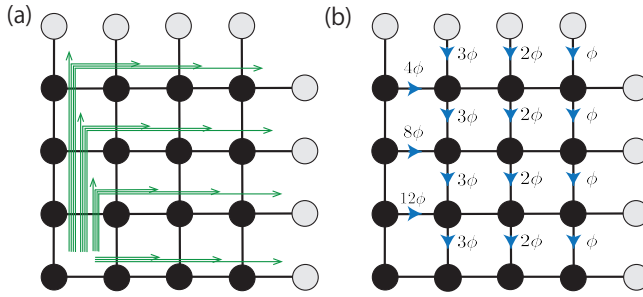


FIG. 1. (Color Online). Sketch of the model and the string gauge for $N_x = N_y = 4$. We impose the periodic boundary condition for x - and y -direction. The green arrows in the right panel represent strings specifying the Peierls phase $\phi_{ij} = 2\pi\phi n_{ij}$. Here, n_{ij} denotes the number of string penetrating the bond connecting sites i and j , and ϕ denotes the flux density $\phi = N_\phi/N_x N_y$. The right panel illustrates the corresponding Peierls phase; when the fermion hops along the blue arrow, it acquires the phase factor ϕ_{ij} . For ϕ is multiple of N_x^{-1} , the string gauge is reduced to the Landau gauge.

atoms, the following two ingredients are essential: non-trivial hopping inducing Landau bands and the repulsive interactions. The former ones are introduced by rotating the system [50–53] or by optically synthesized gauge fields [54]. The repulsive interaction ($V_R > 0$) may be fabricated by a Feshbach resonance [55, 56].

Now, let us take into account the coupling with the environment. The time-evolution of such an open quantum system is governed by the Lindblad equation:

$$\partial_t \rho(t) = -i[H_0, \rho(t)] - \frac{1}{2}\gamma \sum_k \left(L_k^\dagger L_k \rho(t) + \rho(t) L_k^\dagger L_k - 2L_k \rho L_k^\dagger \right), \quad (2)$$

where L_k 's are Lindblad operators describing the loss with the rate $\gamma > 0$. For cold atoms, two-particle loss occurs because of the inelastic scattering [57–63], which is described by setting $L_k \rightarrow c_i c_{i+\mathbf{e}_x}$, $c_i c_{i+\mathbf{e}_y}$. Here $\mathbf{e}_{x(y)}$ denotes the unit vector for each direction, and the lattice constant is set to unity. When we focus on the short-time evolution, the last term describing the quantum-jump is negligible [61–64]. In this case, we can see that the time-evolution is described by

$$\partial_t \rho(t) = -i(H_{\text{eff}} \rho(t) - \rho(t) H_{\text{eff}}^\dagger), \quad (3a)$$

$$H_{\text{eff}} = H_{\text{kin}} + H_{\text{int}}, \quad (3b)$$

with

$$H_{\text{kin}} = - \sum_{\langle i,j \rangle} t_0 e^{i\phi_{ij}} c_i^\dagger c_j, \quad H_{\text{int}} = V \sum_{\langle i,j \rangle} n_i n_j. \quad (3c)$$

We note that the interaction strength takes a complex value; $V = V_R - i\frac{\gamma}{2}$ with $V_R \geq 0$, which makes the Hamiltonian non-Hermitian $H_{\text{eff}} \neq H_{\text{eff}}^\dagger$.

Pseudo-potential approach. — Because treating the large size system is numerically difficult, we simplify the problem with calculating the pseudo-potential [65]. With this approximation, the Hamiltonian is simplified as

$$H'_{\text{eff}} = - \sum_{\langle i,j \rangle} t_0 e^{i\phi_{ij}} \tilde{c}_i^\dagger \tilde{c}_j + V \sum_{\langle i,j \rangle} \tilde{c}_i^\dagger \tilde{c}_j^\dagger \tilde{c}_j \tilde{c}_i, \quad (4a)$$

with

$$H_{\text{kin}} |\phi_\alpha\rangle = |\phi_\alpha\rangle \varepsilon_\alpha, \quad \tilde{c}_i^\dagger = \sum_\alpha' \phi_{i\alpha}^* d_\alpha^\dagger. \quad (4b)$$

Here, $|\phi_\alpha\rangle$ denotes the eigenstate of H_{kin} ($|\phi_\alpha\rangle := \sum_j \phi_{j\alpha} c_j^\dagger |0\rangle$). We label the eigenvalues ε_α so that the relation $\varepsilon_1 \leq \varepsilon_2 \leq \dots$ is satisfied. d_α^\dagger creates the fermion of the eigenstate α . \sum_α' denotes the summation over states satisfying $\varepsilon_\alpha \leq \varepsilon_{N_{\text{keep}}}$; e.g., for $N_{\text{keep}} = N_\phi$ [$N_{\text{keep}} = 2N_\phi$], the summation is taken over the lowest Landau levels (LLs) [the lowest and the second lowest LLs] [66], respectively.

For the numerical computation, we set parameters as $|V| = t_0 = 1$, $\nu = 1/3$, and $N_x = N_y = N$.

Hermitian case. — Here we briefly review the results of the Hermitian system ($\text{Im}V = 0$) for $\nu = 1/3$ where FQH states have been observed. In this case, three-fold degeneracy is observed for the ground state multiplet which is separated by the bulk gap. Computing the Chern number C_{tot} for the ground state multiplet yields $C_{\text{tot}} = 1$, which characterizes the topology of the FQH state with the Hall conductance $\sigma_{xy} = 1/3$. For more details, see Sec. S1 of Supplemental Material [67].

Non-Hermitian case. — Now we introduce the imaginary-part $\text{Im}V < 0$, which makes the system non-Hermitian. Let us start with the definitions of the ground states and the energy gap because the energy spectrum of the non-Hermitian Hamiltonian becomes complex. We define the ground states with the minimum value of the real-part [61]. For our system, these states also have the longest lifetime τ ($\sim -1/\text{Im}E$ with $\text{Im}E < 0$). Correspondingly, the energy gap is defined as $\Delta = \text{Re}E_e - \text{Re}E_g$ which is natural extension of the Hermitian case. Here, E_g (E_e) denotes the energy eigenvalue of the ground state (the first excited state), respectively. In the following, we numerically show that the FQH state survives even under non-Hermiticity by setting $V = \exp(-in_\theta\pi/10)$ with $n_\theta = 0, \dots, 5$.

As a first step, we focus on the case for $n_\theta = 2$. In Fig. 2(a), we plot the energy spectrum E_n where n labels the states such that $\text{Re}E_1 \leq \text{Re}E_2 \leq \dots$ holds. Figure 2(a) indicates that the three-fold degeneracy can be observed even in the presence of non-Hermitian term. The robustness is attributed to many-body translational symmetry, which we discuss below. Besides that, in this figure, we can confirm that the lifetime of the ground states is longer than that of excited states. We note that the energy gap observed in this figure remains finite in the thermodynamic limit, which can be seen in Fig. 2(b).

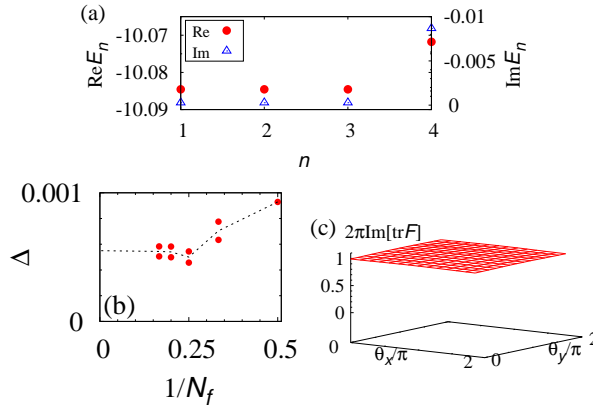


FIG. 2. (Color Online). Numerical results for $n_\theta = 2$ with $V = \exp(-in_\theta\pi/10)$. (a) The real- and the imaginary-part of the energy eigenvalues. The data are obtained for $n_\theta = 2$, $N_\phi = N = 9$, and $N_{\text{keep}} = 2N_\phi$. (b) The bulk gap as a function of N_f . In this plot, the size of the system is chosen so that the flux density $\phi = N_\phi/N^2$ satisfies $1/45 \leq \phi \leq 1/40$. The data of panel (b) are obtained for $N_{\text{keep}} = N_\phi$. However, the difference from the gap for $N_{\text{keep}} = 2N_\phi$ is less than $\delta\Delta \lesssim 10^{-5}t_0$. (c) The imaginary-part of the Berry curvature $\text{tr}F$ as a function of θ_x and θ_y for $N_{\text{keep}} = N_\phi$. For the computation, we divide the two-dimensional space of θ 's into $N_\theta \times N_\theta$ -mesh with $N_\theta = 14$.

From the above numerical results of the bulk gap and the topological degeneracy, one can expect that the FQH phase survives even in the presence of the non-Hermitian term. To confirm this, we address the characterization of the topology of the ground states by computing the many-body Chern number for the non-Hermitian case which is defined as follows:

$$C_{\text{tot}} = \int \frac{d\theta_x d\theta_y}{2\pi i} \text{tr}F(\theta_x, \theta_y), \quad (5a)$$

$$F_{nm}(\theta_x, \theta_y) = \epsilon_{\mu\nu} L \langle \partial_\mu \Psi_n | \partial_\nu \Psi_m \rangle_R. \quad (5b)$$

Here, we have imposed the twisted boundary condition: $c_{N_x+1, i_y}^\dagger = e^{i\theta_x} c_{1, i_y}^\dagger$ and $c_{i_x, N_y+1}^\dagger = e^{i\theta_y} c_{i_x, 1}^\dagger$. The integral is taken over $0 \leq \theta_{x(y)} < 2\pi$, respectively. $F(\theta_x, \theta_y)$ denotes the Berry curvature defined by twisting the boundary conditions. $\partial_\mu := \partial/\partial\theta_\mu$. $\epsilon_{\mu\nu}$ ($\mu, \nu = x, y$) is an anti-symmetric matrix with $\epsilon_{xy} = 1$. $|\Psi_n\rangle_R$ and $L|\Psi_n\rangle$ denote ground states with $n = 1, 2, 3$. The former (latter) ones are right (left) eigenvectors. The summation is taken over repeated indices. We note that the Chern number defined above takes integer (for the proof, see Sec. S2 of Supplemental Material [67]). This fact indicates that the only imaginary-part of the Berry curvature contributes to the Chern number C_{tot} . Employing the method introduced in Refs. [68, 69], we obtain $\text{Im}[\text{tr}F]$. In Fig. 2(b), we can see that the integrand $\text{Im}[\text{tr}F]/2\pi$ becomes almost constant. Evaluating the integration, we obtain $C_{\text{tot}} = 1$.

The above data of the bulk gap, the ground state degeneracy, and the Chern number suggest that the ground

state is topologically identical to the FQH state with $\sigma_{xy} = 1/3$ for the Hermitian case.

In a similar way, we can analyze the system for the other cases of interaction strength. The results are summarized in Fig. 3. This figure indicates that the FQH state observed for $n_\theta = 2$ is adiabatically connected to the one for the Hermitian case; Figures 3(a) and 3(b) show that the bulk gap remains finite with decreasing n_θ ; Figure 3 (c) indicates that the topological properties do not change.

Intriguingly, Fig. 3(b) indicates that the bulk gap opens even for $\text{Re}V = 0$, implying the potential presence of the FQH state without the repulsive interaction. The details of this issue are addressed below.

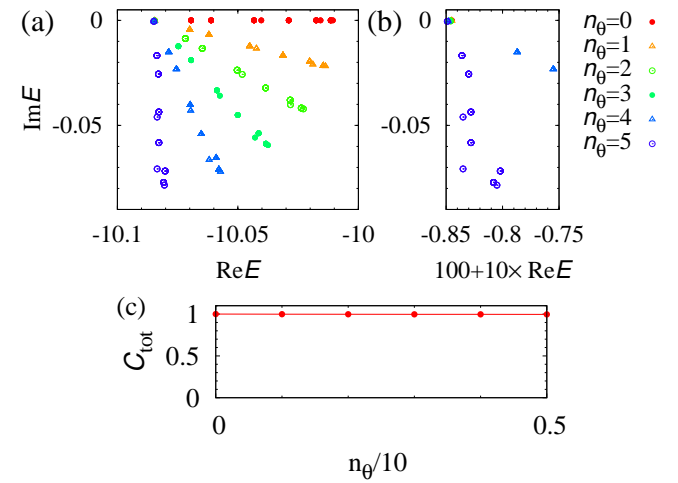


FIG. 3. (Color Online). (a) Energy spectrum for several values of n_θ defining interaction with $V = \exp(-in_\theta\pi/10)$. Panel (b) shows the magnified data. (c) Chern number as a function of n_θ . The data are obtained for $N = 9$ and $N_{\text{keep}} = 18$ where both of the lowest and the second lowest LLs are taken into account. We note that for $n_\theta = 5$ the interaction strength V becomes pure imaginary $V = -i$.

Robustness of the ground state degeneracy against non-Hermitian interactions. — So far, we have numerically observed the three-fold degeneracy of the ground states even in the presence of the non-Hermitian term [see Fig. 2(a) and 3(a)]. This three-fold degeneracy is due to many-body translational symmetry. Namely, the degeneracy multiple of $\nu^{-1} = 2m + 1$ ($m \in \mathbb{Z}$) is observed for arbitrary many-body interaction preserving the translational symmetry. In the following, we discuss the details.

To see this we focus on the case where $N_x = N_y$ and $\phi = n_x/N_x$ ($n_x \in \mathbb{Z}$) holds. Due to the latter condition, the string gauge is reduced to the Landau gauge. In this case, the kinetic term H_{kin} preserves the translation symmetry along the y -axis. Namely, the following condition holds; $T_y H_{\text{kin}} T_y^{-1} = H_{\text{kin}}$ where T_y is the translation operator satisfying $T_y c_{i_x i_y}^\dagger T_y^{-1} = c_{i_x i_y+1}^\dagger$.

Because of the translation symmetry of H_{kin} , one may

take the simultaneous eigenstates of H_{kin} and T_y ;

$$H_{\text{kin}}|\varphi_\alpha(k_y)\rangle = \varepsilon_\alpha|\varphi_\alpha(k_y)\rangle, \quad (6a)$$

$$T_y|\varphi_\alpha(k_y)\rangle = e^{-ik_y}|\varphi_\alpha(k_y)\rangle, \quad (6b)$$

where k_y denotes the momentum along the y -axis ($0 \leq k_y < 2\pi$). Here, let us consider the following gauge transformation: $U_G c_{j_x j_y}^\dagger U_G^\dagger = e^{-i2\pi\phi j_y} c_{j_x j_y}^\dagger$, where U_G is an unitary operator. Applying the gauge transformation to the eigenstate $|\varphi_\alpha(k_y)\rangle$, we obtain

$$T_y U_G |\varphi_\alpha(k_y)\rangle = e^{-i(k_y - 2\pi\phi)} U_G |\varphi_\alpha(k_y)\rangle, \quad (7)$$

which means that applying U_G shifts the momentum by $\Delta k_y := -2\pi\phi$. For the derivation of Eq. (7), see Sec. S3 of Supplemental Material [67].

Eq. (7) elucidates that the many-body translational symmetry results in the degeneracy multiple of ν^{-1} . This can be seen by noticing the following relation

$$\begin{aligned} & \langle \varphi_{\alpha_1}(k_{y1}), \dots, \varphi_{\alpha_{N_f}}(k_{yN_f}) | H_{\text{int}} | \varphi_{\beta_1}(k'_{y1}), \dots, \varphi_{\beta_{N_f}}(k'_{yN_f}) \rangle \\ &= \langle \varphi_{\alpha_1}(k_{y1}), \dots, \varphi_{\alpha_{N_f}}(k_{yN_f}) | U_G^\dagger H_{\text{int}} U_G | \varphi_{\beta_1}(k'_{y1}), \dots, \varphi_{\beta_{N_f}}(k'_{yN_f}) \rangle \\ &= \langle \varphi_{\alpha_1}(k_{y1} + \Delta k_y), \dots, \varphi_{\alpha_{N_f}}(k_{yN_f} + \Delta k_y) | H_{\text{int}} | \varphi_{\beta_1}(k'_{y1} + \Delta k_y), \dots, \varphi_{\beta_{N_f}}(k'_{yN_f} + \Delta k_y) \rangle, \end{aligned} \quad (8)$$

which indicates that the matrix element for the subspace labeled by the total momentum $K = \sum_l k_{yl}$ equals to the one for the subspace labeled by $K' = K + \Delta k_y N_f$. Because the shift of the momentum is rewritten as $\Delta k_y N_f = -2\pi\phi N_f = -2\pi\nu$, we can see that the degeneracy of each eigenvalue is multiple of ν^{-1} .

In the above we have seen the relation between the topological degeneracy and the many-body translational symmetry. In order to support this numerically, we demonstrate that breaking the translational symmetry splits the degeneracy. Specifically, we compute the energy spectrum in the presence of the following disorder

$$H_{\text{dis}} = \sum_i w_i \tilde{c}_i^\dagger \tilde{c}_i, \quad (9)$$

where w_i takes a random value satisfying $-w_0/2 \leq w_i \leq w_0/2$ at each site. In Fig. 4(a) [(b)], the real- [imaginary]-

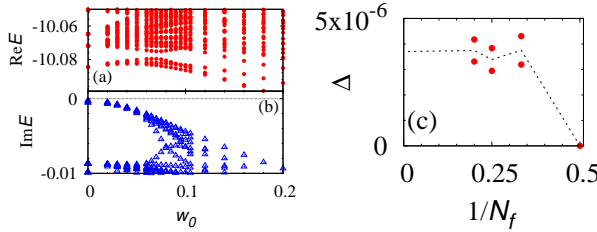


FIG. 4. (Color Online). (a) [(b)] The real- [imaginary-] part of the energy eigenvalues as functions of disorder strength. Turning on disorder w_0 splits the three-fold degeneracy observed for $w_0 = 0$. The data are obtained for $N_\phi = N = 9$ and $n_\theta = 2$ with $V = \exp(-in_\theta\pi/10)$. (c) The bulk gap as a function of N_f which is obtained for H_{ptb} [see Eq. (10)]. Energy difference of the ground state multiplet is of the order of $10^{-13}t_0$ which is much smaller than the energy gap.

part of the energy eigenvalues are plotted against disor-

der strength w_0 , respectively. These figures indicate that breaking the translational symmetry lifts the three-fold degeneracy of the ground states.

The above results indicate that the many-body translational symmetry results in the robustness of topological degeneracy against non-Hermiticity. Our numerical data elucidate that the topological degeneracy can be observed for $1/45 \leq \phi < 1/40$ where the string gauge cannot be reduced to the Landau gauge.

FQH state without the repulsive interaction. — Figures 3(b) and 3(c) imply that the FQH state emerge without the repulsive interaction. In the following, we elucidate the origin of the FQH state for $\text{Re}V = 0$.

Firstly, we point out that the origin of the gap is the interplay between the kinetic term H_{kin} and the non-Hermitian interaction H_{int} (i.e., the mixing between Landau bands). Applying the perturbation theory, we obtain the following Hamiltonian acting on the space spanned by the states in the lowest LLs,

$$H_{\text{ptb}} = P_0 H_{\text{int}} P_0 + P_0 H_{\text{int}} P_1 \frac{1}{E_g^0 - H_{\text{kin}}} P_1 H_{\text{int}} P_0. \quad (10)$$

Here, P_n denotes the projection operator to the subspace where n -fermions are excited to the second lowest LLs. E_g^0 is the ground state energy for $V = 0$. We have omitted the constant term arising from $P_0 H_{\text{kin}} P_0$. Noticing that the prefactor of the last term is $(\text{Im}V)^2/\hbar\omega_0$, we can see that the last term serves as the repulsive interaction. Here $\hbar\omega_0$ denotes the energy gap between the lowest LLs and the second lowest LLs for $V = 0$.

Diagonalizing the effective Hamiltonian (10), we plot the energy gap Δ as a function of N_f in Fig. 4(c). This figure indicates that the energy gap remains finite in the thermodynamic limit. We also note that the three-fold

degeneracy of the ground states is also observed. Thus, one may consider that the gapped state is the FQH state, which is confirmed by the numerical computation yielding $C_{\text{tot}} = 1$ [see Fig. 3(c)].

Therefore, we conclude that the FQH state emerges without the repulsive interaction ($\text{Re}V = 0$) which is adiabatically connected to the FQH state with $\sigma_{xy} = 1/3$ for the Hermitian case.

We stress that the bulk gap opens due to two-body loss inducing the effective repulsive interaction [70], which is reminiscent of the continuous quantum Zeno effect [61–63, 71–75].

Summary and outlook. — In this paper, by focusing on the FQH system at $\nu = 1/3$, we have analyzed impacts of non-Hermiticity on topological ordered phases. We have elucidated the robustness of topological degeneracy against non-Hermitian interactions which arises from many-body translational symmetry. Combining the numerical results of the Chern number $C_{\text{tot}} = 1$ and the topological degeneracy leads us the conclusion that non-Hermitian Hamiltonian (3b) shows the FQH state. Furthermore, we have discovered that the FQH state emerges without repulsive interactions ($\text{Re}V = 0$). This intriguing behavior arises from the effective repulsion induced by the two-body loss, which is reminiscent of the continuous quantum Zeno effect.

We finish this article with comments on future directions. In Fig. 2(d), we have numerically observed that the Berry curvature is almost independent of θ 's, which implies that the computation of the Chern number may be simplified by defining the non-Hermitian counterpart of the one-plaquet Chern number for the Hermitian case [76–79]. We leave the extension of one-plaquet Chern number to non-Hermitian systems as a future work. In addition, we have observed that the interplay between the dissipative two-body interaction and the kinetic term yields four-body interactions which open the bulk gap and yield the FQH state. This unconventional mechanism of gap opening may provide new direction to access exotic topological ordered states induced by many-body interactions higher than two-body (e.g., the Moore-Read state [80, 81]). Hunting such exotic topological ordered states is also left as a significant issue to be addressed.

Acknowledgement. — This work is partly supported by JSPS KAKENHI Grants No. JP16K13845, No. JP17H06138, and No. JP18H05842. A part of numerical calculations were performed on the supercomputer at the ISSP in the University of Tokyo.

[1] D. J. Thouless, M. Kohmoto, M. P. Nightingale, and M. den Nijs, Phys. Rev. Lett. **49**, 405 (1982).
[2] B. I. Halperin, Phys. Rev. B **25**, 2185 (1982).
[3] Y. Hatsugai, Phys. Rev. Lett. **71**, 3697 (1993).
[4] C. L. Kane and E. J. Mele, Phys. Rev. Lett. **95**, 146802 (2005).
[5] C. L. Kane and E. J. Mele, Phys. Rev. Lett. **95**, 226801 (2005).
[6] M. König, S. Wiedmann, C. Brüne, A. Roth, H. Buhmann, L. W. Molenkamp, X.-L. Qi, and S.-C. Zhang, Science **318**, 766 (2007).
[7] X.-L. Qi, T. L. Hughes, and S.-C. Zhang, Phys. Rev. B **78**, 195424 (2008).
[8] M. Z. Hasan and C. L. Kane, Rev. Mod. Phys. **82**, 3045 (2010).
[9] X.-L. Qi and S.-C. Zhang, Rev. Mod. Phys. **83**, 1057 (2011).
[10] D. Pesin and L. Balents, Nature Physics **6**, 376 EP (2010), article.
[11] S. R. Manmana, A. M. Essin, R. M. Noack, and V. Guararie, Phys. Rev. B **86**, 205119 (2012).
[12] T. Yoshida, R. Peters, S. Fujimoto, and N. Kawakami, Phys. Rev. Lett. **112**, 196404 (2014).
[13] T. Yoshida and N. Kawakami, Phys. Rev. B **94**, 085149 (2016).
[14] X.-G. Wen, Advances in Physics **44**, 405 (1995), <https://doi.org/10.1080/00018739500101566>.
[15] D. C. Tsui, H. L. Stormer, and A. C. Gossard, Phys. Rev. Lett. **48**, 1559 (1982).
[16] R. B. Laughlin, Phys. Rev. Lett. **50**, 1395 (1983).
[17] J. K. Jain, Phys. Rev. Lett. **63**, 199 (1989).
[18] E. Tang, J.-W. Mei, and X.-G. Wen, Phys. Rev. Lett. **106**, 236802 (2011).
[19] K. Sun, Z. Gu, H. Katsura, and S. Das Sarma, Phys. Rev. Lett. **106**, 236803 (2011).
[20] T. Neupert, L. Santos, C. Chamon, and C. Mudry, Phys. Rev. Lett. **106**, 236804 (2011).
[21] D. N. Sheng, Z.-C. Gu, K. Sun, and L. Sheng, Nature Communications **2**, 389 EP (2011), article.
[22] N. Regnault and B. A. Bernevig, Phys. Rev. X **1**, 021014 (2011).
[23] E. J. Bergholtz and Z. Liu, International Journal of Modern Physics B **27**, 1330017 (2013), <https://doi.org/10.1142/S021797921330017X>.
[24] A. Kitaev, Annals of Physics **303**, 2 (2003).
[25] A. Kitaev, Annals of Physics **321**, 2 (2006), january Special Issue.
[26] A. Hamma, P. Zanardi, and X.-G. Wen, Phys. Rev. B **72**, 035307 (2005).
[27] T. Takayama, A. Kato, R. Dinnebier, J. Nuss, H. Kono, L. S. I. Veiga, G. Fabbris, D. Haskel, and H. Takagi, Phys. Rev. Lett. **114**, 077202 (2015).
[28] Y. Kasahara, T. Ohnishi, Y. Mizukami, O. Tanaka, S. Ma, K. Sugii, N. Kurita, H. Tanaka, J. Nasu, Y. Motome, T. Shibauchi, and Y. Matsuda, Nature **559**, 227 (2018).
[29] Z. Gong, Y. Ashida, K. Kawabata, K. Takasan, S. Higashikawa, and M. Ueda, Phys. Rev. X **8**, 031079 (2018).
[30] K. Kawabata, K. Shiozaki, M. Ueda, and M. Sato, arXiv preprint arXiv:1812.09133 (2018).
[31] T. Katō, Perturbation theory for linear operators, Vol. 132 (Springer, 1966).
[32] H. Shen, B. Zhen, and L. Fu, arXiv preprint arXiv:1706.07435 (2017).
[33] Y. Xu, S.-T. Wang, and L.-M. Duan, Phys. Rev. Lett. **118**, 045701 (2017).

[34] V. Kozii and L. Fu, arXiv preprint arXiv:1708.05841 (2017).

[35] T. Yoshida, R. Peters, and N. Kawakami, Phys. Rev. B **98**, 035141 (2018).

[36] J. Carlström, M. Stålhammar, J. C. Budich, and E. J. Bergholtz, arXiv preprint arXiv:1810.12314 (2018).

[37] J. C. Budich, J. Carlström, F. K. Kunst, and E. J. Bergholtz, Phys. Rev. B **99**, 041406 (2019).

[38] R. Okugawa and T. Yokoyama, Phys. Rev. B **99**, 041202 (2019).

[39] T. Yoshida, R. Peters, N. Kawakami, and Y. Hatsugai, Phys. Rev. B **99**, 121101 (2019).

[40] H. Zhou, J. Y. Lee, S. Liu, and B. Zhen, Optica **6**, 190 (2019).

[41] K. Kawabata, T. Bessho, and M. Sato, arXiv preprint arXiv:1902.08479 (2019).

[42] T. Yoshida and Y. Hatsugai, arXiv preprint arXiv:1904.10764 (2019).

[43] K. Kimura, T. Yoshida, and N. Kawakami, arXiv preprint arXiv:1905.11761 (2019).

[44] S. Yao and Z. Wang, Phys. Rev. Lett. **121**, 086803 (2018).

[45] S. Yao, F. Song, and Z. Wang, Phys. Rev. Lett. **121**, 136802 (2018).

[46] F. K. Kunst, E. Edvardsson, J. C. Budich, and E. J. Bergholtz, Phys. Rev. Lett. **121**, 026808 (2018).

[47] E. Edvardsson, F. K. Kunst, and E. J. Bergholtz, Phys. Rev. B **99**, 081302 (2019).

[48] D. S. Borgnia, A. J. Kruchkov, and R.-J. Slager, arXiv preprint arXiv:1902.07217 (2019).

[49] Y. Hatsugai, K. Ishibashi, and Y. Morita, Phys. Rev. Lett. **83**, 2246 (1999).

[50] N. K. Wilkin, J. M. F. Gunn, and R. A. Smith, Phys. Rev. Lett. **80**, 2265 (1998).

[51] V. Schweikhard, I. Coddington, P. Engels, V. P. Mogen-dorff, and E. A. Cornell, Phys. Rev. Lett. **92**, 040404 (2004).

[52] N. Cooper, Advances in Physics **57**, 539 (2008), <https://doi.org/10.1080/00018730802564122>.

[53] S. Furukawa and M. Ueda, Phys. Rev. A **86**, 031604 (2012).

[54] Y.-J. Lin, R. L. Compton, K. JimChan nez GarcXue a, J. V. Porto, and I. B. Spielman, Nature **462**, 628 EP (2009).

[55] H. Feshbach, Annals of Physics **5**, 357 (1958).

[56] K. Baumann, N. Q. Burdick, M. Lu, and B. L. Lev, Phys. Rev. A **89**, 020701 (2014).

[57] F. Scazza, C. Hofrichter, M. HDan fer, P. C. De Groot, I. Bloch, and S. FDan lling, Nature Physics **10**, 779 EP (2014), article.

[58] G. Pagano, M. Mancini, G. Cappellini, L. Livi, C. Sias, J. Catani, M. Inguscio, and L. Fallani, Phys. Rev. Lett. **115**, 265301 (2015).

[59] M. Höfer, L. Riegger, F. Scazza, C. Hofrichter, D. R. Fernandes, M. M. Parish, J. Levinsen, I. Bloch, and S. Fölling, Phys. Rev. Lett. **115**, 265302 (2015).

[60] L. Riegger, N. Darkwah Oppong, M. Höfer, D. R. Fernandes, I. Bloch, and S. Fölling, Phys. Rev. Lett. **120**, 143601 (2018).

[61] Y. Ashida, S. Furukawa, and M. Ueda, Phys. Rev. A **94**, 053615 (2016).

[62] M. Nakagawa, N. Kawakami, and M. Ueda, Phys. Rev. Lett. **121**, 203001 (2018).

[63] K. Yamamoto, M. Nakagawa, K. Adachi, K. Takasan, M. Ueda, and N. Kawakami, arXiv preprint arXiv:1903.04720 (2019).

[64] Y. Ashida, S. Furukawa, and M. Ueda, Nature communications **8**, 15791 (2017).

[65] F. D. M. Haldane, Phys. Rev. Lett. **51**, 605 (1983).

[66] For $N_{\text{keep}} = 2N_\phi$, we can take into account effects of Landau band mixing which induces an intriguing phenomena as we see below.

[67] Supplemental Material.

[68] T. Fukui, Y. Hatsugai, and H. Suzuki, Journal of the Physical Society of Japan **74**, 1674 (2005).

[69] T. Fukui and Y. Hatsugai, Journal of the Physical Society of Japan **76**, 053702 (2007).

[70] For $V = V_R > 0$ the prefactor of this term has the opposite sign $[-(\text{Re}V)^2/\hbar\omega_0]$. We have numerically confirmed that the this term suppress the bulk gap for $V = V_R > 0$.

[71] N. Syassen, D. M. Bauer, M. Lettner, T. Volz, D. Dietze, J. J. García-Ripoll, J. I. Cirac, G. Rempe, and S. Dürr, Science **320**, 1329 (2008), <https://science.sciencemag.org/content/320/5881/1329.full.pdf>.

[72] M. J. Mark, E. Haller, K. Lauber, J. G. Danzl, A. Janisch, H. P. Büchler, A. J. Daley, and H.-C. Nägerl, Phys. Rev. Lett. **108**, 215302 (2012).

[73] G. Barontini, R. Labouvie, F. Stubenrauch, A. Vogler, V. Guarrera, and H. Ott, Phys. Rev. Lett. **110**, 035302 (2013).

[74] B. Zhu, B. Gadway, M. Foss-Feig, J. Schachenmayer, M. L. Wall, K. R. A. Hazzard, B. Yan, S. A. Moses, J. P. Covey, D. S. Jin, J. Ye, M. Holland, and A. M. Rey, Phys. Rev. Lett. **112**, 070404 (2014).

[75] T. Tomita, S. Nakajima, I. Danshita, Y. Takasu, and Y. Takahashi, Science Advances **3** (2017), 10.1126/sciadv.1701513, <https://advances.sciencemag.org/content/3/12/e1701513.full.pdf>.

[76] M. B. Hastings and S. Michalakis, Communications in Mathematical Physics **334**, 433 (2015).

[77] T. Koma, arXiv preprint arXiv:1504.01243 (2015).

[78] H. Watanabe, Phys. Rev. B **98**, 155137 (2018).

[79] K. Kudo, H. Watanabe, T. Kariyado, and Y. Hatsugai, Phys. Rev. Lett. **122**, 146601 (2019).

[80] G. Moore and N. Read, Nuclear Physics B **360**, 362 (1991).

[81] M. Greiter, X.-G. Wen, and F. Wilczek, Phys. Rev. Lett. **66**, 3205 (1991).

[82] Q. Niu, D. J. Thouless, and Y.-S. Wu, Phys. Rev. B **31**, 3372 (1985).

[83] F. D. M. Haldane, Phys. Rev. Lett. **55**, 2095 (1985).

[84] D. N. Sheng, X. Wan, E. H. Rezayi, K. Yang, R. N. Bhatt, and F. D. M. Haldane, Phys. Rev. Lett. **90**, 256802 (2003).

[85] K. Kudo, T. Kariyado, and Y. Hatsugai, Journal of the Physical Society of Japan **86**, 103701 (2017), <https://doi.org/10.7566/JPSJ.86.103701>.

Supplemental Materials:
Reduction of topological \mathbb{Z} classification in cold atomic systems

S1. DETAILED RESULTS OF THE HERMITIAN CASE

We here summarize the results of the Hermitian case [16, 18–23, 82–85]. It is well-known that the nearest neighbor interaction ($V > 0$) opens the bulk gap, separating excited states and the ground states whose topological degeneracy is three. Extrapolating the obtained bulk gap for each value of N_f , we can confirm that the bulk gap remains finite in the thermodynamic limit. We can also numerically confirm the three-fold degeneracy for the ground state multiplet [83]. The topological property of the gapped state can be characterized by many-body Chern number C_{tot} with twisting

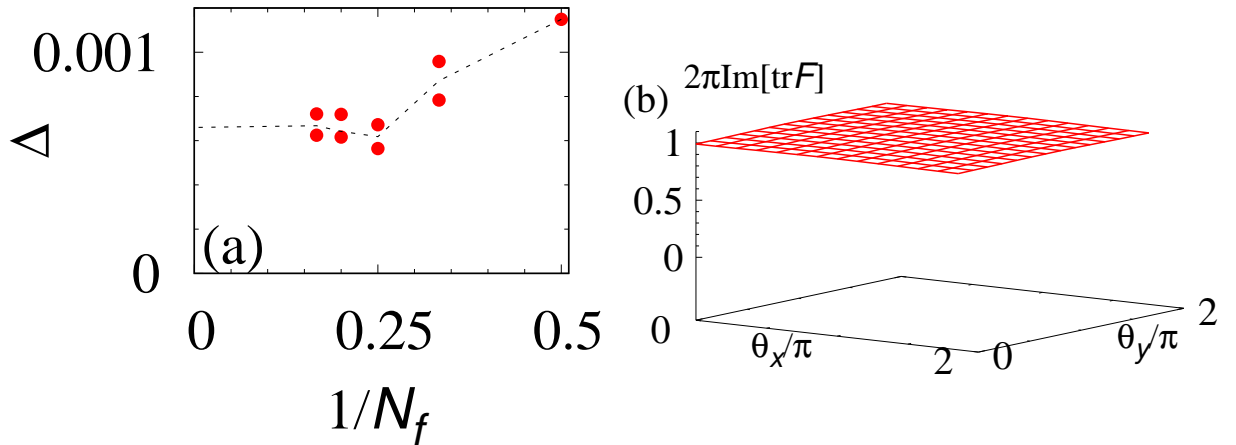


FIG. S1. (Color Online). (a) The bulk gap as a function of N_f for $N_{\text{keep}} = N_\phi$. These data are obtained in a similar way as Fig. 2(a) in the main text. (b) Berry curvature $\text{tr}F/2\pi i$ as a function of θ_x and θ_y .

the boundary condition. Computing the Chern number for the ground state multiplet yields $C_{\text{tot}} = 1$ [84].

The above numerical data indicate that the nearest neighbor interaction $V > 0$ results in the FQH state with $\sigma_{xy} = 1/3$.

S2. CHERN NUMBER AND BERRY CONNECTION

Here, we show that the Chern number defined in Eq. (5b) takes an integer.

Now, consider a two-dimensional parameter space (θ_x, θ_y) with $0 \leq \theta_{x(y)} < 2\pi$. Then, we divide the two-dimensional space into two regions, I and II since taking the unique gauge may not be allowed. Because both of the gauges are available on the boundary of the region I and II, the eigenvectors are related to each other with an invertible matrix M ;

$$|\Psi_n^{II}\rangle_R := |\Psi_{n'}^I\rangle_R M_{n'n}, \quad (\text{S1a})$$

$$_L\langle\Psi_n^{II}| := M_{nn'}^{-1} L\langle\Psi_{n'}^I|, \quad (\text{S1b})$$

where the summation is taken over repeated indices.

Let us evaluate the integration of Eq. (5b). Applying Stokes' theorem, we can rewrite it as

$$C_{\text{tot}} = \frac{1}{2\pi i} \int_C d\theta \cdot (\text{tr}A^I - \text{tr}A^{II}), \quad (\text{S2a})$$

with

$$A_{nm}^\alpha = _L\langle\Psi_n^\alpha| \nabla \Psi_m^\alpha\rangle_R. \quad (\text{S2b})$$

Here, the integral of Eq. (S2a) is taken along the boundary. $d\theta := (d\theta_x, d\theta_y)$, and $\nabla := (\partial/\partial\theta_x, \partial/\partial\theta_y)$.

Eq. (S2a) can be further simplified as follows:

$$\begin{aligned}
C_{\text{tot}} &= \frac{1}{2\pi i} \int_C d\boldsymbol{\theta} \cdot \text{tr} (M^{-1} \nabla M) \\
&= \frac{1}{2\pi i} \int_C d\boldsymbol{\theta} \cdot \nabla \text{tr} \log M \\
&= \frac{1}{2\pi i} \int_C d\boldsymbol{\theta} \cdot \nabla \log \det M.
\end{aligned} \tag{S3}$$

Noticing that $\det M$ is a single-valued function, we can see that the integral is reduced to the winding number

$$\begin{aligned}
C_{\text{tot}} &= \frac{1}{2\pi} \text{Im} \int_C d\boldsymbol{\theta} \cdot \nabla \log \det M, \\
&\in \mathbb{Z}.
\end{aligned} \tag{S4}$$

Therefore, we can conclude that the Chern number takes integer.

S3. DERIVATION OF EQ. (7)

As mentioned in the main text, Eq. (7) can be obtained for the Landau gauge with $N_x = N_y$.

As a preparation, we discuss the translational symmetry in term of the eigenvectors (3b). The state $|\varphi_\alpha(k_y)\rangle$ can be expanded as

$$|\varphi_\alpha(k_y)\rangle = \sum_{i_x, i_y} \varphi_{i_x i_y \alpha} c_{i_x i_y}^\dagger |0\rangle. \tag{S5}$$

Because $|\varphi_\alpha(k_y)\rangle$ is an eigenstate of T_y [see Eq. (6)], we have

$$\varphi_{i_x i_y -1 \alpha} = e^{-ik_y} \varphi_{i_x i_y \alpha}. \tag{S6}$$

Now we show that Eq. (7) holds. This can be seen by analysing whether $U_G |\varphi_\alpha(k_y)\rangle$ is an eigenstate of T_y ;

$$\begin{aligned}
T_y U_G |\varphi_\alpha(k_y)\rangle &= \sum_{j_x=1}^{N_x} \sum_{j_y=1}^{N_y} e^{-i2\pi\phi j_y} T_y \varphi_{j_x j_y \alpha} c_{j_x j_y}^\dagger |0\rangle \\
&= \sum_{j_x=1}^{N_x} \sum_{j_y=1}^{N_y} e^{-i2\pi\phi j_y} \varphi_{j_x j_y \alpha} c_{j_x j_y +1}^\dagger |0\rangle \\
&= \sum_{j_x=1}^{N_x} \sum_{j_y=2}^{N_y+1} e^{-i2\pi\phi(j_y-1)} \varphi_{j_x (j_y-1) \alpha} c_{j_x j_y}^\dagger |0\rangle \\
&= \sum_{j_x=1}^{N_x} \sum_{j_y=2}^{N_y+1} e^{-i2\pi\phi(j_y-1) - ik_y} \varphi_{j_x j_y \alpha} c_{j_x j_y}^\dagger |0\rangle \\
&= \sum_{j_x=1}^{N_x} e^{-ik_y} \left[\sum_{j_y=1}^{N_y} e^{-i2\pi\phi(j_y-1)} \varphi_{j_x j_y \alpha} c_{j_x j_y}^\dagger |0\rangle + (e^{-i2\pi\phi N_y} - 1) \varphi_{j_x 1 \alpha} c_{j_x 1}^\dagger |0\rangle \right] \\
&= e^{-i(k_y - 2\pi\phi)} U_G |\varphi_\alpha(k_y)\rangle.
\end{aligned} \tag{S7}$$

Here, from the third to the fourth line we have used Eq. (S6). From fifth to the last line, we have used the

relation $\phi N_y = 1$ which is satisfied for the system with the Landau gauge and for $N_x = N_y$.